Dipole-forbidden atomic transitions induced by superintense x-ray laser fields

Aleksander Skjerlie Simonsen* and Morten Førre†
Department of Physics and Technology, University of Bergen, N-5007 Bergen, Norway
(Received 11 March 2016; published 27 June 2016)

A hydrogen atom, initially prepared in the $2s$ and/or $2p(m = \pm 1)$ states, is assumed irradiated by 0.8 keV (1.5 nm) photons in pulses of 1–250 fs duration and intensities in the range 10^{20} to 10^{23} W/cm^2. Solving the corresponding time-dependent Schrödinger equation from first principles, we show that the ionization and excitation dynamics of the laser-atom system is strongly influenced by interactions beyond the electric dipole approximation. A beyond-dipole two-photon Raman-like transition between the $2s$ and $2p(m = \pm 1)$ states is found to completely dominate the underlying laser-matter interaction. It turns out that the large difference in the ionization rates of the $2s$ and $2p(m = \pm 1)$ states is important in this context, effectively leading to a symmetry breaking in the corresponding (beyond-dipole) bound-bound dynamics with the result that a net population transfer between the states occurs throughout the laser-matter interaction period. Varying the x-ray exposure time as well as the laser intensity, we probe the phenomenon as the bound wave packet oscillates between having $2s$ and $2p(m = \pm 1)$ character, eventually giving rise to a Rabi-like oscillation pattern in the populations.

DOI: 10.1103/PhysRevA.93.063425

I. INTRODUCTION

The question of how atoms and molecules interact with laser light has received wide interest since the invention of the laser in 1960. Due to the ever increasing number of both temporally and spatially focused coherent photons that can be delivered by such light sources, lasers have become the ideal tool for controlling, observing, and manipulating systems at the quantum level. With the development of exceedingly powerful pulses of femto- and attosecond duration and wavelengths entering the x-ray regime, laser imaging techniques have approached the level of temporal and spatial resolution needed to resolve the motion of bound electrons in atomic and molecular systems [1].

The peak brilliance of xuv [2,3] and x-ray [4–6] lasers has increased by several orders of magnitude due to ongoing development of state-of-the-art facilities based on the free-electron laser (FEL) technology. With the launch of new machines penetrating deep into the x-ray regime, like, e.g., the hard-x-ray free-electron laser (XFEL), the Linac Coherent Light Source (LCLS) at SLAC (Stanford), and the European XFEL that is under construction at DESY in Hamburg, the electronic response of single atoms and molecules exposed to ultraintense x rays of unprecedented high intensity and short wavelength is open for exploration [7,8]. X-ray lasers represent powerful tools for probing dynamics and structure down to atomic scales [9]. At laser intensities beyond 10^{17} W/cm^2 and with keV photons, nonlinear behavior is expected to become prominent which in turn poses significant challenges to theoretical modeling, numerical simulation, and interpretation of experimental results, thus calling for accurate theoretical descriptions of the light-matter interaction at the fundamental level [10–12]. In this context, nonlinear ionization of neon exposed to intense x rays at photon energies exceeding 1 keV has been studied experimentally [13]. Furthermore, the deep inner-shell multiphoton multiple ionization dynamics of xenon by 5.5 keV photons [14], as well as the process of direct two-photon absorption in germanium with 5.6 keV XFEL radiation [15], were observed with laser pulses from the SACLA facility in Japan [6].

The European XFEL will provide ultraintense x-ray pulses at 0.05–4.7 nm wavelength. With such short wavelengths and high intensities, the validity of the frequently applied dipole approximation becomes questionable [12]. In the dipole approximation, it is assumed that the laser field can be described by a homogeneous time-varying electric field, i.e., any dependence on spatial coordinates as well as the entire magnetic field have been neglected. This approximation is usually justified for systems being exposed to electromagnetic radiation of wavelengths much larger than the length scale of the target in question [16], and when the laser intensity is weak enough so that magnetic-field-induced effects can safely be neglected. Hence the dipole formulation of the light-matter interaction is likely to break down in the limit of extremely intense [17–22] and ultrahigh-frequency fields [12,23,24].

Using a recently developed Hamiltonian for the light-matter interaction beyond the dipole approximation [11], we solve the three-dimensional time-dependent Schrödinger equation for a hydrogen atom interacting with an ultraintense and z-polarized 0.8 keV (1.5 nm) x-ray laser beam of varying duration (1–250 fs) and intensity. It is found that, for laser intensities beyond 10^{20} W/cm^2 and for targets prepared in excited states prior to illumination, the laser-matter interaction is strongly influenced by magnetic-field-induced nondipole dynamics. Starting out in, for example, the hydrogenic $2s$, $2p(m = 1)$, and/or $2p(m = -1)$ states, clear evidence of transitions between these degenerate states are exhibited in the final state. Moreover, the mixing of the states follows a periodic pattern with respect to the x-ray exposure time, giving rise to Rabi-like oscillations characterized by periodic population inversions and revivals of the initial state. Note that for the z-polarized laser field considered here $2s \leftrightarrow 2p(m = \pm 1)$ transitions are strictly forbidden in the dipole approximation, and as such the dynamics is of beyond-dipole nature and highly nonperturbative. To this end, the underlying (nondipole) process is of nonlinear character and is mainly governed by the

*aleksander.simonsen@uib.no
†morten.forre@uib.no

direct absorption and emission of two photons in a Raman-type transition.

II. THEORY

In the nonrelativistic limit, the temporal evolution of a hydrogenic wave packet Ψ in a laser field is governed by the time-dependent Schrödinger equation (TDSE), $i\hbar\partial_t\Psi = H\Psi$, where H is the light-atom interaction Hamiltonian. Assuming propagating (transverse) fields, the laser pulse is conveniently defined in terms of the vector potential $\boldsymbol{A}(\eta)$ and the scalar potential $\phi(\eta)$ with $\eta = \omega t - \boldsymbol{k}\cdot\boldsymbol{r}$, ω and $\boldsymbol{k} = \frac{\omega}{c}\hat{\boldsymbol{k}}$ being the angular frequency and wave vector of the electromagnetic radiation, respectively. Performing a *gauge* transformation on the potentials, i.e., letting the potentials transform according to the rules $\boldsymbol{A} \to \boldsymbol{A}' = \boldsymbol{A} + \nabla\xi$ and $\phi \to \phi' = \phi - \partial_t\xi$, where ξ is an arbitrary differentiable function depending on the Lorentz scalar η [25,26], the corresponding electric ($\boldsymbol{E} = -\nabla\phi - \partial_t\boldsymbol{A} = -\nabla\phi' - \partial_t\boldsymbol{A}'$) and magnetic ($\boldsymbol{B} = \nabla\times\boldsymbol{A} = \nabla\times\boldsymbol{A}'$) fields are left unchanged. Following our recent work [11], we let the potentials transform according to

$$\xi(\boldsymbol{r},t) = \xi(\eta) = \sum_{j=1}^{\infty} a_j \frac{mc^2}{q\omega}\int_{-\infty}^{\eta}\left[\frac{q\boldsymbol{A}(\eta')}{mc}\right]^{2j} d\eta', \quad (1)$$

where $m = m_e$ and $q = -e$ are the mass and charge of the electron, and the coefficient $a_j = (2j)!/[4^j(2j-1)(j!)^2]$. Assuming the potentials $\boldsymbol{A}$ and ϕ fulfill the Coulomb (or radiation) gauge condition ($\nabla\cdot\boldsymbol{A} = 0$, $\phi = 0$), then the minimal-coupling Hamiltonian, $H = \frac{1}{2m}(\boldsymbol{p} - q\boldsymbol{A}')^2 + q\phi' + V$, transforms into [11]

$$H = \frac{\boldsymbol{p}^2}{2m} + V - \frac{q}{m}\boldsymbol{A}\cdot\boldsymbol{p} + \frac{c}{2}\sum_{j=1}^{\infty} a_j\left\{\left(\frac{q\boldsymbol{A}}{mc}\right)^{2j}, \hat{\boldsymbol{k}}\cdot\boldsymbol{p}\right\} + \lim_{n\to\infty}\frac{mc^2}{2}\sum_{j=1}^{n}\left(\frac{q\boldsymbol{A}}{mc}\right)^{2(n+j)}\sum_{i=1}^{n-j+1} a_{j+i-1}a_{n-i+1}, \quad (2)$$

where $V = V(\boldsymbol{r})$ is the Coulomb potential, and curly brackets denote the anticommutator $\{a,b\} = ab + ba$. Provided that the condition $|q\boldsymbol{A}|/m < c$ holds, i.e., the velocity of the corresponding classical (free) particle in the field is never allowed to exceed the speed of light, the last (double) sum in Eq. (2) vanishes identically and the Hamiltonian is cast into the final *propagation gauge* form [11],

$$H = \frac{\boldsymbol{p}^2}{2m} + V - \frac{q}{m}\boldsymbol{A}\cdot\boldsymbol{p} + \frac{c}{2}\sum_{j=1}^{\infty} a_j\left\{\left(\frac{q\boldsymbol{A}}{mc}\right)^{2j}, \hat{\boldsymbol{k}}\cdot\boldsymbol{p}\right\}. \quad (3)$$

Note that the transformed potentials $\boldsymbol{A}' = \boldsymbol{A} + \nabla\xi$ and $\phi' = \phi - \partial_t\xi$ both become nonzero and that $\boldsymbol{A}'$ contains a longitudinal component. Still, the four-vector $A'^{\mu} = (\phi'/c, \boldsymbol{A}')$ satisfies the Lorentz gauge condition, $\partial_\mu A'^{\mu} = 0$.

Any beyond-dipole (nondipole) response of the hydrogenic system is manifested due to either the spatial variations in the vector potential $\boldsymbol{A}$ and/or the homogeneous component of $\boldsymbol{A}$ through the last term in Eq. (3). This latter term is also responsible for the radiation pressure force acting upon the electron throughout the laser pulse. The force is due to the intimate interplay between the electric- and magnetic-field components of the laser, effectively giving rise to a push of the electronic wave packet in the laser propagation direction [17–19,27,28]. Assuming $|q\boldsymbol{A}|/m \ll c$, i.e., the electron is not allowed to attain relativistic velocities in the laser field, then all the higher-order terms but the first one in the series expansion in Eq. (3) may be neglected. Furthermore, assuming the long-wavelength approximation (LWA) [16] on the laser field, i.e., taking $\boldsymbol{A}$ to be a purely time-dependent function, then the Hamiltonian (3) simplifies to

$$H \simeq \frac{\boldsymbol{p}^2}{2m} + V - \frac{q}{m}\boldsymbol{A}_0\cdot\boldsymbol{p} + \frac{c}{2}\left(\frac{q\boldsymbol{A}_0}{mc}\right)^2\hat{\boldsymbol{k}}\cdot\boldsymbol{p}, \quad (4)$$

with $\boldsymbol{A}_0 \equiv \boldsymbol{A}(t)$.

The Hamiltonian (4) has the same form as the one used in [11,28–32]. In the more standard approach, the beyond-dipole Hamiltonian is obtained by expanding the vector potential in powers of $1/c\ \hat{\boldsymbol{k}}\cdot\boldsymbol{r}$ around $\eta = \omega t$. Substituting $\boldsymbol{A}(\eta) = \boldsymbol{A}_0(t) - 1/c\ \frac{d\boldsymbol{A}_0}{dt}\hat{\boldsymbol{k}}\cdot\boldsymbol{r} + \cdots$ into the usual minimal coupling Hamiltonian, imposing the Coulomb gauge restriction on $\boldsymbol{A}$, and omitting terms proportional to $1/c^2$ or higher, yield the following standard laser-matter interaction Hamiltonian:

$$H' = \frac{1}{2m}(\boldsymbol{p} - q\boldsymbol{A})^2 + V \quad (5)$$

$$= \frac{\boldsymbol{p}^2}{2m} + V - \frac{q}{m}\boldsymbol{A}_0\cdot\boldsymbol{p} + \frac{q^2}{2m}\boldsymbol{A}_0^2 + \frac{q}{mc}\left(-q\boldsymbol{A}_0\cdot\frac{d\boldsymbol{A}_0}{dt} + \frac{d\boldsymbol{A}_0}{dt}\cdot\boldsymbol{p}\right)\hat{\boldsymbol{k}}\cdot\boldsymbol{r} + O(1/c^2). \quad (6)$$

It has been found that the last (nondipole) term in the Hamiltonian, which is proportional to $\partial_t\boldsymbol{A}_0\cdot\boldsymbol{p}$, can be neglected in the high-intensity regime [12,28,33–36], and Eq. (6) is effectively cast into the approximate form

$$H' \simeq \frac{\boldsymbol{p}^2}{2m} + V - \frac{q}{m}\boldsymbol{A}_0\cdot\boldsymbol{p} + \frac{q^2}{2m}\boldsymbol{A}_0^2 - \frac{q^2}{mc}\boldsymbol{A}_0\cdot\frac{d\boldsymbol{A}_0}{dt}\hat{\boldsymbol{k}}\cdot\boldsymbol{r}. \quad (7)$$

Although derived by different means, Eq. (4) is mathematically equivalent to Eq. (7), and the former can be derived from the latter by applying the unitary (gauge) transformation

$$\Psi = U\Psi', \quad (8)$$

$$H = UH'U^{\dagger} + i\hbar\dot{U}U^{\dagger}, \quad (9)$$

with [11,28–32]

$$U = \exp\left[-i\frac{q^2}{2mc\hbar}\boldsymbol{A}_0^2(t)\hat{\boldsymbol{k}}\cdot\boldsymbol{r} + i\frac{q^2}{2m\hbar}\int_{-\infty}^{t}\boldsymbol{A}_0^2(t')dt' + i\frac{q^4}{8m^3c^2\hbar}\int_{-\infty}^{t}\boldsymbol{A}_0^4(t')dt'\right]. \quad (10)$$

When comparing the two forms of the beyond-dipole laser-atom formulations as represented by the Hamiltonians (4) and (7), respectively, it is found that the former represents a powerful tool for investigating nondipole ionization dynamics induced by intense laser fields [11]. Although they are mathematically equivalent, independent simulations with

the respective Hamiltonians yield identical results only if the problem is handled within an exact treatment—and since *any* numerical discretization involves at least some level of approximation (truncation), one formulation may be the better choice. The comparison is similar to the choice between the length-gauge and the velocity-gauge forms of the dipole interaction Hamiltonian. It is found that with the Hamiltonian (4), a converged solution to the TDSE is usually achieved at a comparatively smaller truncation limit in the wave-function expansion, in particular in terms of angular basis functions [11].

III. RESULTS AND DISCUSSION

We will now make use of the Hamiltonians (4) and (7) in a study of nondipole-assisted multiphoton ionization of excited hydrogen atoms exposed to superintense x-ray fs laser fields. In the following work, we have applied both the Hamiltonians (4) and (7) in order to ensure convergence and gauge invariance of the results. The z-polarized laser pulse is modeled as $\boldsymbol{A}_0(t) = \frac{E_0}{\omega} f(t)\sin(\omega t)\hat{\boldsymbol{z}}$, where E_0 is the electric-field strength at peak intensity, and $f(t)$ defines the pulse profile which is assumed to be of sine-square shape. The time-dependent Schrödinger equation is solved by expanding the corresponding state vector in a set of both bound and continuum hydrogenic states. For details about our numerical representation of the problem, readers are referred to Ref. [33]. The combination of very high continuum electron energies and laser pulses of relatively long duration makes this a particularly challenging computational problem. Therefore, an absorbing boundary was imposed on the edges of the numerical grid in order to avoid unphysical reflections. The convergence of the results was checked by varying the grid sizes in the simulations.

The top panel in Fig. 1 shows the ionization probability of the hydrogenic $2s$ state as a function of the duration of the laser field. The x-ray radiation is taken to have a wavelength of 1.5 nm corresponding to the photon energy 0.8 keV, and the peak laser intensity is set to $I_0 = 5.6 \times 10^{21}$ W/cm^2. Results obtained with the nondipole Hamiltonian (4) are compared with the corresponding dipole approximation results, as obtained by neglecting the last (nondipole) term in Eq. (4). Within the dipole approximation, the ionization yield can easily be fitted with an exponential function, and as such a well-defined ionization rate may be ascribed to the process. The beyond-dipole result, on the other hand, follows a much more complex pathway. First, the ionization yield exhibits a narrow peak (maximum) in the short-pulse limit where the laser-matter interaction is predominantly characterized by nonadiabatic excitation and ionization processes [37]. Second, in the long-pulse regime the ionization probability features a rather nontrivial dependency on the pulse duration.

The explanation for the odd behavior of the nondipole ionization yield in the limit of long pulses can be found by inspecting the bound-state population dynamics. The survival probability of the initial state is depicted in the middle panel of Fig. 1. Noteworthy is that the population of the $2s$ state exhibits an oscillatory behavior—in clear contrast to the dipole signal which instead follows a simple exponential decay law. Furthermore, the collapse and revival of the initial state follows a periodic cycle with respect to the x-ray exposure time, with an oscillation period of about 100 fs. In order to

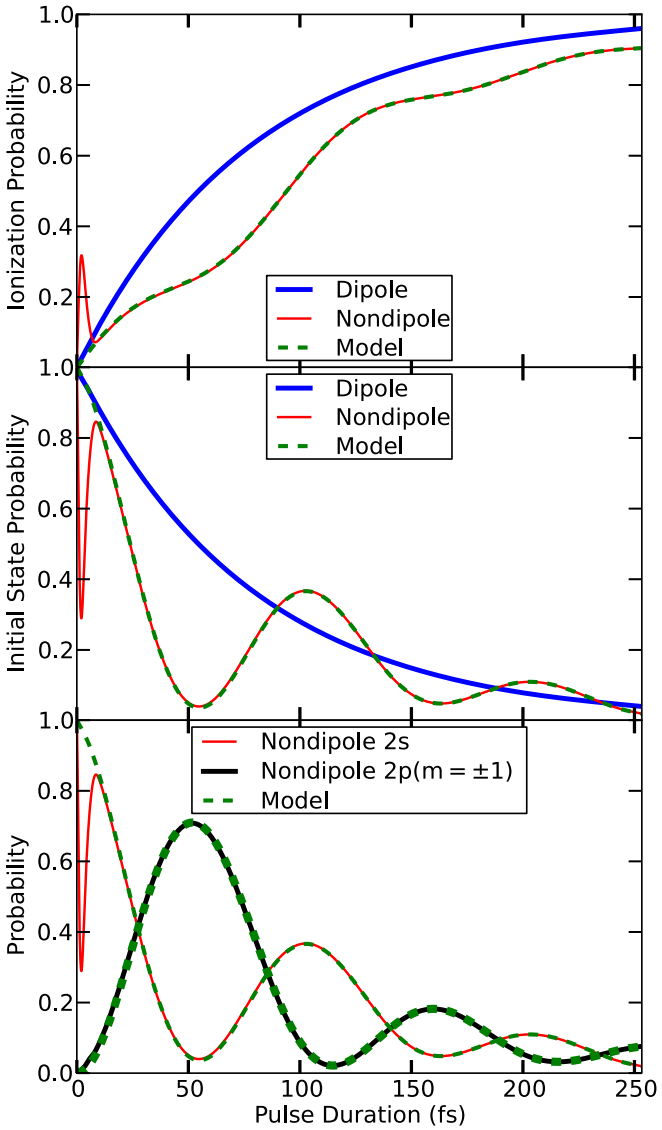

FIG. 1. Hydrogen initially prepared in the $2s$ state and exposed to a 0.8 keV x-ray pulse of peak intensity $I_0 = 5.6 \times 10^{21}$ W/cm^2. Top and middle panel: probability of ionization (top panel) and initial-state survival probability (middle panel) vs laser-pulse duration, as obtained in the dipole (thick blue line) and nondipole (red line) limits, respectively. Bottom panel: the populations in the $2s$ (red line) and $2p(m = \pm 1)$ (thick black line) states. In all panels, results obtained with the simple model (11) are depicted in dashed (green) lines.

reveal the mechanism behind this peculiar observation, we consider the population distribution among the other bound states. Due to the narrow spectral width associated with the nearly monochromatic light source, the $2p(m = \pm 1)$ states represent the only two candidates which might support a significant population. Note, however, that the $2s \rightarrow 2p(m = \pm 1)$ transition is strictly forbidden in the dipole approximation, and, as such, it can only take place in the presence of the nondipole field.

The bottom panel in Fig. 1 shows the total population in the $2p(m = \pm 1)$ states as a function of the laser-pulse duration. For symmetry reasons the population is evenly

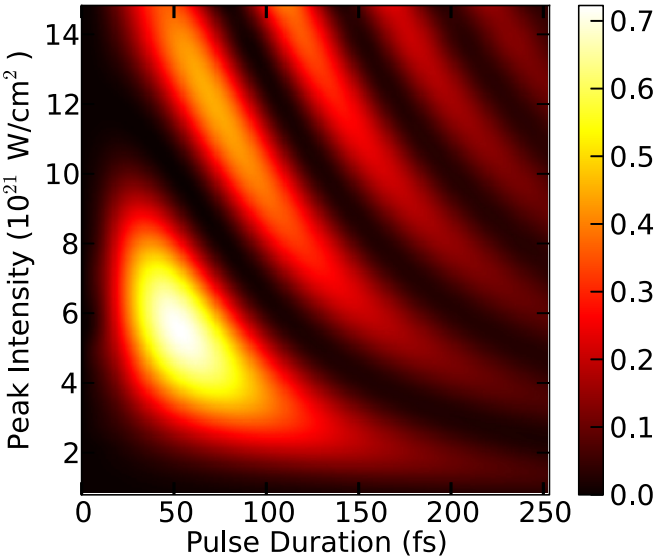

FIG. 2. As Fig. 1 (bottom panel), but a 2D map of the final-state probability in the $2p(m = \pm 1)$ states as a function of both the laser-pulse duration and intensity.

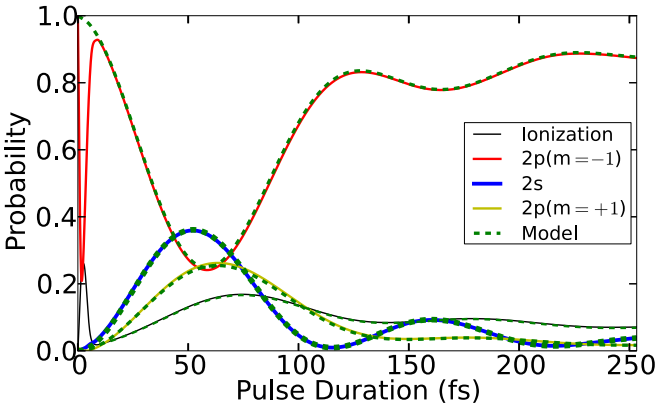

FIG. 3. Hydrogenic $2p(m = -1)$ state interacting with 0.8 keV fs x-ray pulses of intensity $I_0 = 5.6 \times 10^{21}$ W/cm^2. Populations in the $2p(m = -1)$ (red line), $2s$ (thick blue line), $2p(m = +1)$ (yellow line), and the ionization yield (thin black line) vs laser-pulse duration. Results obtained with the simple model (11) are depicted in dashed (green) lines.

distributed among the $m = \pm 1$ channels. The population in the $2s$ is also depicted for comparison. As it turns out, the periodic pattern of the $2s$ state probability is followed by corresponding oscillations in the $2p(m = \pm 1)$ population, as is clearly manifested in the bottom panel of Fig. 1. As seen in the figure, the respective oscillation amplitudes are successively damped with increasing irradiation time simply due to the increasing ionization yield.

Because of the centrifugal barrier, the $2p(m = \pm 1)$ states are significantly more resistant to ionization than the $2s$ state, making them effectively transparent to the x-ray radiation. Hence once the radiation pressure associated with the beyond-dipole dynamics causes the bound electron to be pushed into a mixed $2s$-$2p$ configuration, the atom becomes temporarily more resistant to ionization. This is consistent with the nondipole ionization yield (Fig. 1, top panel) exhibiting fringes in its incline, thus obstructing the existence of a well-defined ionization rate.

Figure 2 shows a 2D map of the variation of the $2p(m = \pm 1)$ population with respect to both the laser illumination time and intensity. As apparent from the figure, the Rabi-like oscillations in the $2p(m = \pm 1)$ probability are expressed over a wide range of intensities beyond 10^{20} W/cm^2. Obviously, the corresponding Rabi oscillation period varies with the laser intensity, i.e., it shortens with increasing brilliance. In the low-intensity limit, nondipole effects are of less importance and the $2s \leftrightarrow 2p(m = \pm 1)$ transition dynamics eventually loses its significance. As a matter of fact, the mechanism responsible for the coherent population dynamics among excited (degenerate) states is manifested throughout the x-ray regime, as well as for other choices of initial states. In order to demonstrate this, the corresponding results obtained with the $2p(m = -1)$ initial state are shown in Fig. 3. The pulse characteristics are the same as in Fig. 1, and indeed a similar dependency on the laser-pulse duration is exhibited, in that the evolution is characterized by Rabi oscillations. Nevertheless, here the picture is somewhat more complex in that a secondary transition to the $2p(m = +1)$ state is allowed, thus partially prohibiting population inversions and revivals in the system.

The underlying physics behind the $2s$-$2p$ population dynamics can be explained by means of a simple model as formulated by the model Hamiltonian

$$H_{\text{model}} = \frac{\boldsymbol{p}^2}{2m} + V - \frac{q}{m}\boldsymbol{A}_0 \cdot \boldsymbol{p} - \frac{q^2}{2mc}\left(\frac{E_0}{\omega}\right)^2 f(t)\dot{f}(t) \times [|2s\rangle\langle 2s|\hat{\boldsymbol{k}} \cdot \boldsymbol{r}|2p, m = 1\rangle\langle 2p, m = 1| + \text{H.a.} \times |2s\rangle\langle 2s|\hat{\boldsymbol{k}} \cdot \boldsymbol{r}|2p, m = -1\rangle\langle 2p, m = -1| + \text{H.a.}]. \tag{11}$$

Here H.a. stands for the Hermitian adjoint operator. In the simple model, only two nondipole couplings are retained, i.e., the couplings between the $2s$ and $2p(m = \pm 1)$ states, as represented by the projection operators in Eq. (11). Note that all other nondipole interaction terms are neglected entirely. The dipole interaction, on the other hand, is still fully accounted for within the model framework. Note further that the nondipole interaction operator is here formulated within the so-called *envelope approximation* as was developed in a recent work [32]. Solving the time-dependent Schrödinger equation with the Hamiltonian (11), it is found that in the limit of long pulses, the laser-atom dynamics is accurately captured by this comparably simple model, as is clearly illustrated by the comparisons made between (approximate) model and *ab initio* results in Figs. 1 and 3, respectively.

The model (11) effectively serves as a means for exploring the underlying mechanism responsible for the observed bound-bound state population dynamics. Within the *envelope approximation* [32] the beyond-dipole component of the laser field varies so slowly with respect to time that it may be considered quasistatic. As such, the $2s$ and $2p(m = \pm 1)$ states become temporarily mixed in the nondipole field. Now, without the additional dipole component of the field, this population mixing is only transient and would vanish at the end of the laser

interaction. The large difference in the (dipole) ionization rates of the $2s$ and $2p(m = \pm 1)$ states is, however, important in this context, effectively leading to an asymmetry in the respective $2s$ and $2p(m = \pm 1)$ populations. It is this symmetry-breaking mechanism that is responsible for the net population transfer between the states throughout the illumination period. As such, the $2s \leftrightarrow 2p$ transitions are governed by the intimate interplay between the magnetic-field-induced dressing of the bound states and dipole-driven (nonlinear) multiphoton absorption and emission processes.

IV. CONCLUSION AND SUMMARY

To summarize, we have investigated x-ray-induced photoionization of excited hydrogen atoms by ultrahigh-intensity fs laser pulses. Our findings indicate that the beyond-dipole component of the laser-matter interaction plays a decisive role in the underlying dynamics. Starting out in, for example, the $2s$ and/or $2p(m = \pm 1)$ excited states initially, clear evidence of population mixing between these bound states is exhibited in the final state. Since this $2s \leftrightarrow 2p$ transition is strictly forbidden in the dipole approximation *per se*, it can only occur due to the mutual interplay between the electric- (dipole) and magnetic- (nondipole) field components of the laser, in a Raman-type two-photon transition. One consequence of this is that the ionization yield of the total system reveals a nontrivial dependence on the laser exposure time, simply due to the asymmetry in the corresponding ionization yields of the $2s$ and $2p$ states, effectively making the system temporarily more transparent or opaque to the x rays. As a final remark, we point out that the nondipole phenomenon discovered here is of general validity and applies to almost any quantum system prepared in degenerate (excited) states exposed to x rays of unprecedented intensity, and that from an experimental point of view, the relative population of the $2s$ and $2p(m = \pm 1)$ states can be readily measured by exploiting the large difference in their respective fluorescence lifetimes.

ACKNOWLEDGMENT

This work was supported by the Bergen Research Foundation (Norway).

[1] F. Krausz and M. Ivanov, Rev. Mod. Phys. **81**, 163 (2009).
[2] W. Ackermann, G. Asova, V. Ayvazyan, A. Azima, N. Baboi, J. Bahr, V. Balandin, B. Beutner, A. Brandt, A. Bolzmann *et al.*, Nat. Photon. **1**, 336 (2007).
[3] T. Shintake, H. Tanaka, T. Hara, T. Tanaka, K. Togawa, M. Yabashi, Y. Otake, Y. Asano, T. Bizen, T. Fukui *et al.*, Nat. Photon. **2**, 555 (2008).
[4] S. Jamison, Nat. Photon. **4**, 589 (2010).
[5] P. Emma, R. Akre, J. Arthur, R. Bionta, C. Bostedt, J. Bozek, A. Brachmann, P. Bucksbaum, R. Coffee, F.-J. Decker *et al.*, Nat. Photon. **4**, 641 (2010).
[6] T. Ishikawa, H. Aoyagi, T. Asaka, Y. Asano, N. Azumi, T. Bizen, H. Ego, K. Fukami, T. Fukui, Y. Furukawa *et al.*, Nat. Photon. **6**, 540 (2012).
[7] L. Young, E. P. Kanter, B. Krässig, Y. Li, A. M. March, S. T. Pratt, R. Santra, S. H. Southworth, N. Rohringer, L. F. DiMauro *et al.*, Nature (London) **466**, 56 (2010).
[8] B. Rudek, S.-K. Son, L. Foucar, S. W. Epp, B. Erk, R. Hartmann, M. Adolph, R. Andritschke, A. Aquila, N. Berrah *et al.*, Nat. Photon. **6**, 858 (2012).
[9] G. Dixit, J. M. Slowik, and R. Santra, Phys. Rev. Lett. **110**, 137403 (2013).
[10] A. Sytcheva, S. Pabst, S.-K. Son, and R. Santra, Phys. Rev. A **85**, 023414 (2012).
[11] M. Førre and A. S. Simonsen, Phys. Rev. A **93**, 013423 (2016).
[12] H. Bachau, M. Dondera, and V. Florescu, Phys. Rev. Lett. **112**, 073001 (2014).
[13] G. Doumy, C. Roedig, S.-K. Son, C. I. Blaga, A. D. DiChiara, R. Santra, N. Berrah, C. Bostedt, J. D. Bozek, P. H. Bucksbaum *et al.*, Phys. Rev. Lett. **106**, 083002 (2011).
[14] H. Fukuzawa, S.-K. Son, K. Motomura, S. Mondal, K. Nagaya, S. Wada, X.-J. Liu, R. Feifel, T. Tachibana, Y. Ito *et al.*, Phys. Rev. Lett. **110**, 173005 (2013).
[15] K. Tamasaku, E. Shigemasa, Y. Inubushi, T. Katayama, K. Sawada, H. Yumoto, H. Ohashi, H. Mimura, M. Yabashi, K. Yamauchi *et al.*, Nat. Photon. **8**, 313 (2014).
[16] H. R. Reiss, Phys. Rev. A **22**, 770 (1980).
[17] H. R. Reiss, Phys. Rev. A **87**, 033421 (2013).
[18] H. R. Reiss, Phys. Rev. Lett. **26**, 1072 (1971).
[19] M. Førre, J. P. Hansen, L. Kocbach, S. Selstø, and L. B. Madsen, Phys. Rev. Lett. **97**, 043601 (2006).
[20] M. Førre, S. Selstø, J. P. Hansen, and L. B. Madsen, Phys. Rev. Lett. **95**, 043601 (2005).
[21] C. T. L. Smeenk, L. Arissian, B. Zhou, A. Mysyrowicz, D. M. Villeneuve, A. Staudte, and P. B. Corkum, Phys. Rev. Lett. **106**, 193002 (2011).
[22] C. I. Moore, A. Ting, S. J. McNaught, J. Qiu, H. R. Burris, and P. Sprangle, Phys. Rev. Lett. **82**, 1688 (1999).
[23] H. R. Varma, M. F. Ciappina, N. Rohringer, and R. Santra, Phys. Rev. A **80**, 053424 (2009).
[24] M. Dondera and H. Bachau, Phys. Rev. A **85**, 013423 (2012).
[25] H. R. Reiss, Phys. Rev. A **89**, 022116 (2014).
[26] H. R. Reiss, arXiv:1510.07034v2.
[27] N. J. Kylstra, R. A. Worthington, A. Patel, P. L. Knight, J. R. Vázquez de Aldana, and L. Roso, Phys. Rev. Lett. **85**, 1835 (2000).
[28] J. R. Vázquez de Aldana, N. J. Kylstra, L. Roso, P. L. Knight, A. Patel, and R. A. Worthington, Phys. Rev. A **64**, 013411 (2001).
[29] M. Y. Emelin and M. Y. Ryabikin, Phys. Rev. A **89**, 013418 (2014).
[30] M. Y. Ryabikin and A. M. Sergeev, Opt. Express **7**, 417 (2000).
[31] A. V. Kim, M. Y. Ryabikin, and A. M. Sergeev, Phys. Usp. **42**, 54 (1999).
[32] A. S. Simonsen, T. Kjellsson, M. Førre, E. Lindroth, and S. Selstø, Phys. Rev. A **93**, 053411 (2016).
[33] M. Førre and A. S. Simonsen, Phys. Rev. A **90**, 053411 (2014).
[34] M. Førre, Phys. Rev. A **74**, 065401 (2006).
[35] K. J. Meharg, J. S. Parker, and K. T. Taylor, J. Phys. B **38**, 237 (2005).
[36] A. Bugacov, M. Pont, and R. Shakeshaft, Phys. Rev. A **48**, R4027 (1993).
[37] A. S. Simonsen and M. Førre, Phys. Rev. A **92**, 013405 (2015).